Analytica Chimica Acta 829 (2014) 15–21

Contents lists available at ScienceDirect

Analytica Chimica Acta

journal homepage: www.elsevier.com/locate/aca

Prussian blue–gold nanoparticles-ionic liquid functionalized reduced graphene oxide nanocomposite as label for ultrasensitive electrochemical immunoassay of alpha-fetoprotein

Qi Gao, Na Liu, Zhanfang Ma *

Department of Chemistry, Capital Normal University, Beijing, 100048, China

HIGHLIGHTS

- IL-rGO-Au-PDDA-PB nanocomposites were fabricated and used as a signal tag.
- Ionic liquid functionalized reduced graphene oxide was used as a substrate.
- An immunosensor was designed for AFP based on signal amplification.
- This method performed very well on the detection of clinical serum specimens.

GRAPHICAL ABSTRACT

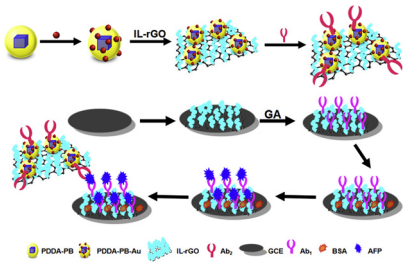

ARTICLE INFO

Article history:
Received 26 December 2013
Received in revised form 17 April 2014
Accepted 21 April 2014
Available online 26 April 2014

Keywords:
Ionic liquid functionalized reduced graphene oxide
Prussian blue
Alpha-fetoprotein
Electrochemical immunosensor

ABSTRACT

In this work, poly(diallyldimethylammonium chloride) (PDDA) protected Prussian blue/gold nanoparticles/ionic liquid functionalized reduced graphene oxide (IL-rGO-Au-PDDA-PB) nanocomposite was fabricated. The resulting nanocomposite exhibited high biocompatibility, conductivity and catalytic activity. To assess the performance of the nanocomposite, a sensitive sandwich-type immunosensor was constructed for detecting alpha-fetoprotein (AFP). Greatly enhanced sensitivity for this immunosensor was based on triple signal amplification strategies. Firstly, IL-rGO modified electrode was used as biosensor platform to capture a large amount of antibody due to its increased surface area, thus amplifying the detection response. Secondly, a large number of Au-PDDA-PB was conjugated on the surface of IL-rGO, which meant the enrichment of the signal and the more immobilization of label antibody. Finally, the catalytic reaction between H_2O_2 and the IL-rGO-Au-PDDA-PB nanocomposite further enhanced the signal response. The signals increased linearly with AFP concentrations in the range of 0.01–100 ng mL^{-1}. The detection limit for AFP was 4.6 pg mL^{-1}. The immunosensor showed high sensitivity, excellent selectivity and good stability. Moreover, the immunosensor was applied to the analysis of AFP in serum sample with satisfactory result.

1. Introduction

Highly sensitive and reliable detection of cancer marker is currently the important subject of cancer diagnosis [1–3]. Alpha-fetoprotein (AFP) is an important tumor marker for the early diagnosis of the patients with hepatic carcinoma, nasopharyngeal cancer and epithelial ovarian tumors [4,5]. Various

* Corresponding author. Tel.: +86 1068902491.
E-mail address: mazhanfang@cnu.edu.cn (Z. Ma).

http://dx.doi.org/10.1016/j.aca.2014.04.045
0003-2670/

techniques and methods have been used for the early detection of AFP [6–9]. Immunosensors, particularly the electrochemical immunosensors, have become the predominant analytical technique due to their high sensitivity, wide liner range, low cost and ease of miniaturization [10–12]. Moreover, the sandwich-type electrochemical immunosensors have gained much attention because of their high sensitivity based on the signal amplification strategies [13,14].

More recently, it is attractive to develop graphene nanocomposites as enhancers to constructing electrochemical immunosensor because these nanocomposites can produce a synergic effect among conductivity, catalytic activity, and biocompatibility and further realize the signal amplification [15,16]. Many efforts have been made to the fabrication of graphene nanocomposites [17–19]. On the other hand, Prussian blue (PB) has been widely used as an electron transfer mediator for analytical applications [20,21]. Particularly, it was denoted as an "artificial peroxidase" because of its rapid catalytic rate toward the reduction of hydrogen peroxide (H_2O_2) at low overpotential [22]. As a result, graphene-PB nanocomposites have gained extensive attention in the field of biosensors due to its electrocatalysis, low cost and convenient preparation [23,24].

The fabrication of graphene-PB nanocomposites was generally based on two approaches: (1) The PB nanoparticles (PBNPs) were grown on the surface of graphene sheets through in situ reduction reaction [25,26]. (2) The PBNPs were chemically pre-synthesized and later mixed with graphene [27]. However, in the first approach, the reduced graphene sheets tend to form irreversible aggregation in aqueous solutions and prevent the direct assembly of the negative charged PBNPs because of its residual negative charge. Hence, the uniformity and morphology of PBNPs on graphene are hardly controlled. The main problem associated with the second approach is the size of PBNPs can not be easily controlled because the small solubility product constant of PB ($K_{sp} = 3.3 \times 10^{-41}$) [28,29]. In electrochemical application, the uniformity and the size of PBNPs are crucial for the catalytic performance [30]. Therefore, it is still a challenge to develop a new strategy that controls the uniformity and size of PBNPs on graphene to realize high catalytic activity and stability of graphene-PB nanocomposites.

In this work, we chose positive poly(diallyldimethylammonium chloride) (PDDA) as the stabilizer to control the growth and handle the agglomeration of PBNPs. More importantly, AuNPs modified PBNPs (Au-PB) were synthesized because they possessed higher catalytic activity and redox biocompatibility compared with the pure PBNPs and AuNPs [31]. On the other hand, our group reported the synthesis of Au-ionic liquid functionalized reduced graphene oxide nanocomposite (Au-IL-rGO) and was employed as a substrate material for the immobilization of capture antibody [32]. We found that the IL-rGO integrated both the excellent conductivity of graphene, hydrophilicity of ionic liquid and large specific surface. Hence, in this work, Au-PDDA-PB was conjugated on the surface of IL-rGO to obtain the novel IL-rGO-Au-PDDA-PB nanocomposites. The resulting nanocomposite exhibited favorable conductivity, catalytic activity and biocompatibility. To assess the performance of the nanocomposite, a sensitive sandwich-type immunosensor was constructed for detecting AFP. Greatly enhanced sensitivity for this immunosensor was based on triple signal amplification strategies. The IL-rGO modified electrode was used as immunosensing platform because it could not only facilitate the electrons transfer but also provide a large accessible surface area for the immobilization of antibody. A large number of Au-PDDA-PB was conjugated on IL-rGO to realize the signal enrichment of the immunosensing probe and the further catalysis amplification was employed by reducing H_2O_2 by the IL-rGO-Au-PDDA-PB nanocomposites. The proposed immunosensor showed high sensitivity and wide linear detection response for AFP. Moreover, the proposed method was successfully applied for the detection of AFP in human serum sample.

2. Experimental

2.1. Materials

IL-NH_2 (e.g., 1-aminopropyl-3-methylimidazoliumchloride) was from Shanghai Chenjie Chemical Co. Ltd. (Shanghai, China). GO was obtained from JCNANO (Nanjing, China). PDDA (35% (w/w) aqueous solution) was achieved from Sigma–Aldrich. Sodium citrate, urea acid (UA), NaH_2PO4, Na_2HPO_4, KCl, KOH, C_2H_5OH, H_2O_2, acetone, albumin from bovine serum (BSA), glutaraldehyde (GA), potassium ferricyanide ($K_3Fe(CN)_6$) and $FeCl_2{\cdot}4H_2O$ were purchased from Beijing Chemical Reagents Company (Beijing, China). Hydrogen tetrachloroaurate hydrate ($HAuCl_4{\cdot}xH_2O$, 99%), D-(+)-glucose, sodium borohydride ($NaBH_4$), ascorbic acid (AA) were achieved from Alfa Aesar. Mouse monoclonal anti-AFP (Ab_1, Catalog: L1C301) and mouse monoclonal anti-AFP (Ab_2, Catalog: L1C302) were used as capture antibody and label antibody, respectively. The two kinds of anti-AFP and AFP (source: human fetal cord serum) were purchased from Linc-Bio Company (Shanghai, China). Carcinoembryonic antigen (CEA) was purchased from Biosynthesis Biotechnology Company (Beijing, China). Human immunoglobulin G (IgG) was purchased from Chengwen Biological Company (Beijing, China). The clinical human samples were from the Capital Normal University Hospital. All the reagents were of analytical grade and used as received. Ultrapure water (resistivity > 18 $M\Omega\,cm^{-2}$) was used throughout the experiments.

2.2. Apparatus

Transmission electron microscopy (TEM) was performed with a JEOL-100CX electron microscope (Hitachi, Japan) under 80 kV accelerating voltage. X-ray photoelectron spectroscopy (XPS) analysis of the samples was performed with ESCALAB 250 X-ray photoelectron spectroscope (Thermofisher, American). Electrochemical measurements were carried out on CHI-832 electrochemical workstation (Chenhua, China). A three-electrode system was used in the experiment with a glassy carbon electrode (GCE) (4 mm in diameter) as the working electrode, an Ag/AgCl electrode (saturated KCl) and a Pt wire electrode as reference electrode and counter electrode, respectively.

2.3. Synthesis of AuNPs

AuNPs with the size of 5 nm were synthesized according to the as-reported method [33]. The 5 nm AuNPs were prepared at room temperature by adding 1 mL 1% sodium citrate solution to 100 mL 0.01% $HAuCl_4$ solution with stirring. After 1 min, 1.6 mL 0.075% $NaBH_4$ (dissolved in 1% sodium citrate solution) was added. The solution immediately turned red, indicating the formation of AuNPs.

2.4. Synthesis of PDDA-PB

PDDA-PB nanoparticles were synthesized according to the literature with a little modification [34]. Briefly, 10 mL of 10 mM $K_3Fe(CN)_6$ was slowly added to 10 mL of 10 mM $FeCl_2{\cdot}4H_2O$ containing 0.4% PDDA under vigorous stirring at room temperature. After the addition, the reaction mixture turned dark blue immediately, indicating the formation of PBNPs. Then acetone was added into the resulting solutions to precipitate the PBNPs and remove the residual KCl. The resultant precipitate was centrifuged at 10,000 rpm for 10 min and washed with acetone and water for

several times. Finally, the resultant precipitate was re-dispersed in 4 mL water.

2.5. Synthesis of Au-PDDA-PB nanocomposite

500 μL aqueous solution of PDDA-PB was added to 20 mL aqueous suspension of the obtained 5 nm AuNPs under vigorous stirring at room temperature for 4 h. The resultant was centrifuged at 8000 rpm for 10 min and re-dispersed in 3 mL water. The product was stored at 4 °C before use.

2.6. Synthesis of IL-rGO

IL-rGO was synthesized according to our previous work [32]. Briefly, 10 g IL-NH_2 was added into 50 mL of GO homogeneous dispersion in water (0.5 mg mL^{-1}), then 50 mg KOH was added into the above solution, and then the mixture was subjected to ultrasonication for 30 min. Finally, the homogeneous solution was vigorously stirred at 80 °C for 24 h. The resulting IL-rGO was subsequently centrifuged, washed with ethanol and ultrapure water, and re-dispersed in ultrapure water (1 mg mL^{-1}).

2.7. Synthesis of IL-rGO-Au-PDDA-PB nanocomposites

The IL-GO (1 mg mL^{-1}) was subjected to ultrasonication for 15 min before use. Then, 500 μL IL-GO was added to the 3 mL suspension of Au-PDDA-PB nanocomposite. The mixture was kept at room temperature with stirring for overnight. The resultant was centrifuged at 8000 rpm for 10 min and re-dispersed in 1 mL water.

2.8. Fabrication of immunosensing probe

The immunosensing probe was prepared by immobilizing label anti-AFP (Ab_2) on to the surface of IL-rGO-Au-PDDA-PB nanocomposite. Briefly, the nanocomposite was dispersed in 1 mL of 0.01 M phosphate buffer (PB) (pH 7.0). Subsequently, Ab_2 (100 μL, 1 mg mL^{-1}) was added into the dispersion and gently mixed for 12 h. After centrifugation, the IL-rGO-Au-PDDA-PB-Ab_2 nanocomposites were blocked by BSA (1.0 wt%) for 2 h to avoid any non-specific absorption. After centrifuged and washed for several times, the obtained IL-rGO-Au-PDDA-PB-Ab_2 nanocomposite was re-dispersed in 1 mL of 0.01 M PB (pH 7.0) and stored at 4 °C before use.

2.9. Preparation of the immunosensor

The GCE was polished repeatedly using alumina powder and then thoroughly cleaned before use. After that, 20 μL of the prepared IL-rGO was dropped onto GCE and then dried in air. To immobilize the anti-AFP onto the electrode surface, 40 μL of GA (2.5%, v/v) solution was dropped onto the IL-rGO modified electrode surface and incubated for 1 h. Subsequently, the obtained electrode was incubated with capture anti-AFP (Ab_1) (200 μg mL^{-1}, pH 7.0) at 4 °C overnight. Finally, the anti-AFP modified electrode was incubated in a solution of BSA (1.0 wt%) for 1 h at room temperature to block possible remaining active sites and avoid non-specific adsorption. After each step, the electrode was thoroughly washed with 0.01 M PBS (pH 7.0) to remove physically absorbed species. The proposed immunosensor was stored at 4 °C when not in use.

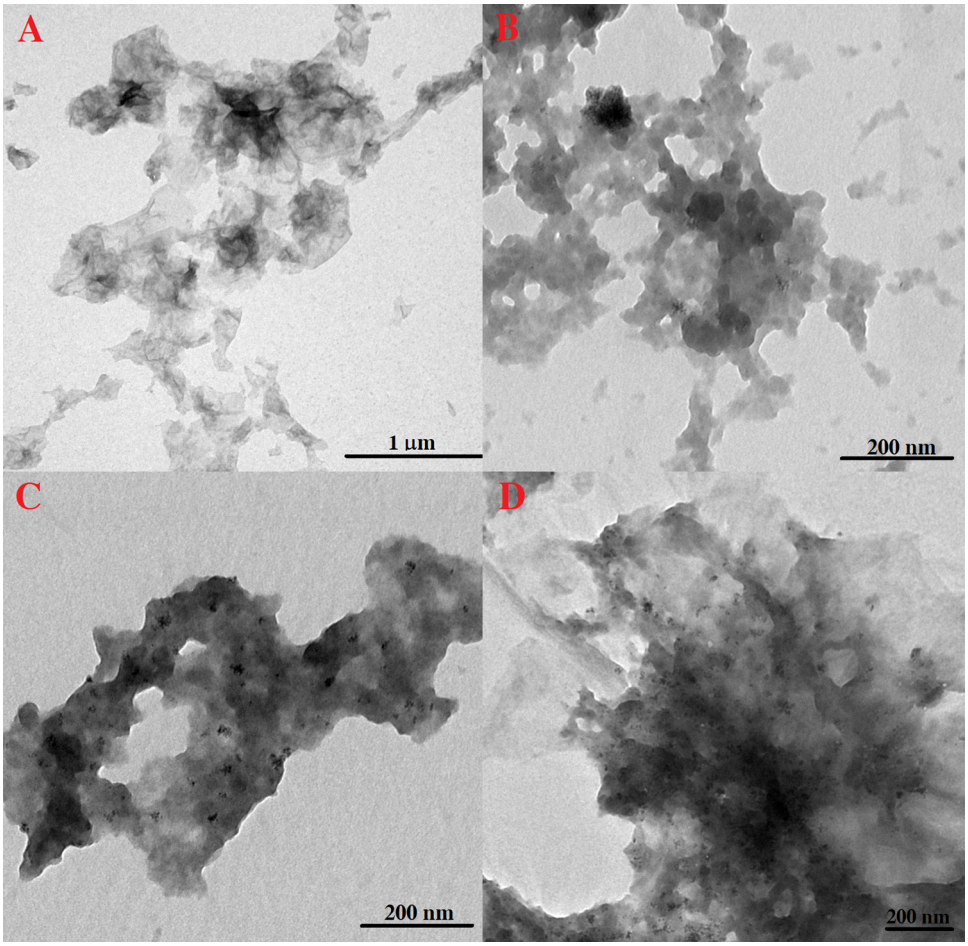

Fig. 1. TEM images of (A) IL-rGO, (B) PDDA-PB, (C) Au-PDDA-PB, (D) IL-rGO-Au-PDDA-PB nanocomposite.

2.10. Electrochemical detection of AFP

The electrochemical measurements were based on a sandwich-type immunoassay. Before measurement, anti-AFP modified electrodes were incubated with various concentrations of AFP for 40 min at 37 °C and then washed with PB (pH 7.0). Then, the prepared IL-rGO-Au-PDDA-PB-Ab_2 buffer solution was dropped onto the electrode surface and incubated for another 1 h. After washing, the square wave voltammogram (SWV) was performed from −0.2 to 0.6 V in 0.1 M PBS (pH 6.5) containing 4 mM H_2O_2.

3. Results and discussion

3.1. Characterizations of immunosensing matrix and probe

Fig. 1A shows the typical TEM image of IL-rGO, which exhibits transparent and wrinkled sheets. The IL-rGO shows good dispersion in aqueous solution. XPS spectra are performed on GO and IL-rGO in supporting information (Fig. S1). As shown in Fig. S1C, there is an addition component at 285.9 eV, which can be assigned to the C—N groups from the imidazolium ring of the ionic liquid [35]. Besides, the N1s appears at 401.8 eV, with a lower binding energy shoulder at 399.7 eV, obviously confirming the presence of IL-NH_2 units on IL-GS (Fig. S1D) [36]. These results indicate that the IL-rGO is successfully synthesized which is consistent with our previous report [32]. Fig. 1(B–D) shows the TEM images of the as-prepared PDDA-PB, Au-PDDA-PB, IL-rGO-Au-PDDA-PB nanocomposites, respectively. The PDDA-PB nanoparticles are belt shaped and about 20–30 nm in width. After the negatively changed AuNPs are added into the positively charged PDDA-PB nanoparticles, small black dots are observed in the PDDA-PB matrix, indicating the formation of PDDA-PB-Au nanocomposite. After the reaction between the amine groups of IL-rGO and AuNPs on the surface of Au-PDDA-PB nanocomposite, it can be seen that lots of Au-PDDA-PB are densely deposited on the surface of IL-rGO, indicating the formation of IL-rGO-Au-PDDA-PB nanocomposite. XPS analyses provide detailed information on the chemical composition of the as-prepared nanocomposite. The fully scanned spectrum demonstrates that Fe2p, C1s, N1s and O1s exist in PDDA-PB sample (Fig. S2A). To further understand the electronic state of the elements, the higher-resolution spectrum is displayed (Fig. S2B). The binding energy of $Fe2p_{3/2}$ and $Fe2p_{1/2}$ are observed at 712.1 and 721.1 eV respectively, which originate from the presence of Fe^{3+}. The peak at 708.1 eV can be assigned to $Fe2p_{3/2}$ of $FeCl_2$ [37]. It can be conclude that the PBNPs are successfully synthesized. The appearance of Au 4f on the Au-PDDA-PB sample is consistent with the Au^0 state (Fig. S2C), confirming the presence of AuNPs on the surface PDDA-PB [36]. The XPS peaks for C1s, N1s, O1s, Fe2p and Au4f core level regions can be obviously observed in Fig. S2D. Thus, these results confirm the formation of PDDA-PB, Au-PDDA-PB, IL-rGO-Au-PDDA-PB nanocomposites.

3.2. Principle of the proposed immunoassay

The schematic illustration of the stepwise immunosensor fabrication is shown in Scheme 1. Au-PDDA-PB nanocomposite was synthesized by the electrostatic interaction between the positive PDDA-PB and the negative AuNPs. Then, the Au-PDDA-PB nanocomposite was conjugated onto IL-rGO through the amine groups of IL-rGO and AuNPs. The AuNPs on the nanocomposite can increase the specific surface area to capture a large amount of antibodies. With the sandwich-type assay format, the antigen–antibody immunocomplex was formed on the surface of the IL-rGO modified electrode. Greatly enhanced sensitivity for this immunosensor was based on triple signal amplification strategies: (1) IL-rGO was used as biosensor platform due to its increased surface area to capture a large amount of anti-AFP, thus amplifying the detection response. (2) A large number of Au-PDDA-PB was conjugated on the surface of IL-rGO, which meant the enrichment of the signal and the more immobilization of capture antibody. (3) The catalytic reaction between the H_2O_2 and the IL-rGO-Au-PDDA-PB nanocomposite further enhanced the signal response.

3.3. Characterization of the immunosensor

The DPV measurements were used to monitor the electrochemical behavior of the modification procedure after each step. As shown in Fig. 2A, the current of IL-rGO modified electrode (curve b) was higher than that of a bare GCE (curve a), which was attributed to the excellent electronic transport properties. When

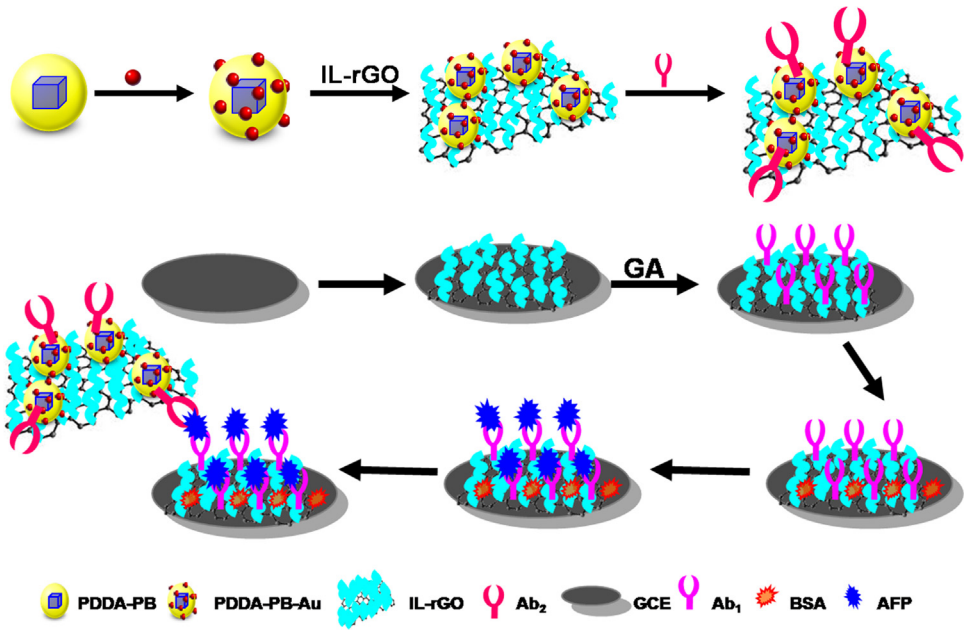

Scheme 1. The fabrication processes of the signal tag and the electrochemical immunosensor.

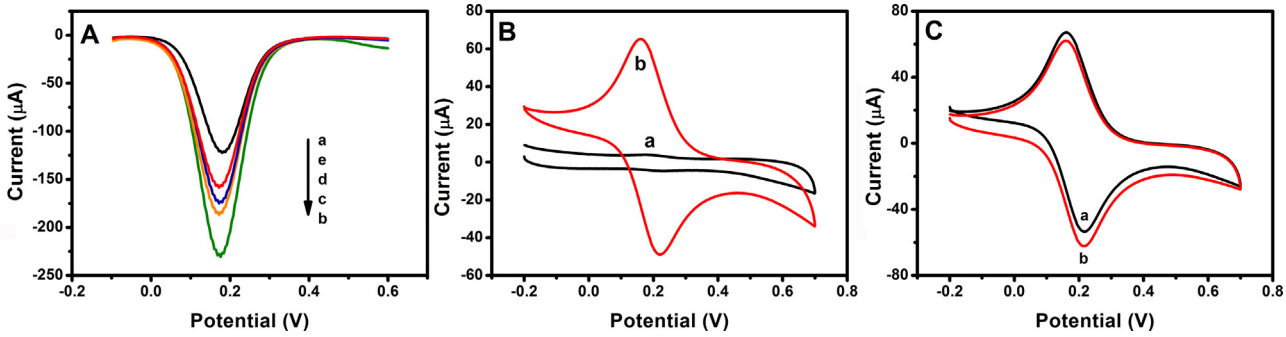

Fig. 2. (A) DPV performed in PBS-$[Fe(CN)_6]4-/3-$: (a) bare GCE; (b) IL-rGO modified GCE electrode; (c) anti-AFP/IL-rGO modified GCE electrode; (d) BSA/anti-AFP/IL-rGO modified GCE electrode; (e) modified GCE after incubation with 10 ng mL^{-1} AFP. (B) CVs of the proposed immunosensor before (a) and after (b) incubated with excess with immunosensing probe in PBS, pH 6.5. (C) CVs of the immunosensor in 0.1 M PBS (pH 6.5) without H_2O_2 (a) and with 4 mM H_2O_2 (b).

anti-AFP was immobilized onto the IL-rGO modified electrode via cross-linking with GA, there was an obvious decrease of the current due to the formation of an electron-blocking layer (curve c). Subsequently, the current response further decreased after blocked with BSA (curve d) and incubated in a solution in 10 ng mL^{-1} AFP (curve e), which was ascribed to the insulating protein layers on the electrode retarding the electron transfer. According to the results, the IL-rGO-modified electrode could be used for the detection of AFP.

Significantly, the signal amplification performance of the sensor was monitored by CV experiments. No redox peaks were observed due to the lack of a redox-active substance (Fig. 2B, curve a). After the sandwich immunoreaction, a pair of stable and well-defined redox peaks were observed at 0.16 and 0.22 V (Fig. 2B, curve b), indicating the successful immobilization of the immunosensing probe on the surface of the electrode. After an addition of 4 mM H_2O_2 into the PBS, an obvious catalytic process was observed with the increase of cathodic peak and the decrease of anodic peak (Fig. 2C). The results showed that the signal was greatly amplified because of the excellent catalytic performance. The electrochemical catalysis of PB for H_2O_2 could be explained as follows [34]:

$$2K_2Fe^{II}[Fe^{II}(CN)_6] + H_2O_2 + 2H^+ = 2KFe^{III}[Fe(CN)_6] + 2H_2O + 2K^+ \quad (1)$$

$$KFe^{III}[Fe(CN)_6] + K^+ + e^- = K_2Fe^{II}[Fe^{II}(CN)_6] \quad (2)$$

3.4. Optimization of the experimental parameters of the immunosensor

The pH and incubation time are two important parameters in the immunoreaction. The pH influenced the electrochemical behavior of PB and the activity of the proteins. The responses increased with increasing pH values from 5.0 to 6.5, but then decreased as the pH increased further (Fig. S3A). Consequently, the optimal pH of 6.5 was chosen in later studies. The currents to AFP increased with incubation time and then started to level off at 40 min (Fig. S3B). Hence, an incubation time of 40 min was selected for the immunoassay.

3.5. Evaluation of repeatability, specificity and stability of the immunosensor

In order to evaluate the repeatability of the immunosensor, five freshly prepared modified electrodes were incubated with AFP (1 ng mL^{-1}). All five electrodes exhibited similar response behavior, and the relative standard deviation (RSD) was 3.2%. This demonstrated that the repeatability of the proposed immunosensor for AFP was acceptable.

To further investigate the specificity of the immunosensor, the modified electrodes were incubated with AFP (10 ng mL^{-1}) containing 100 ng mL^{-1} of different interfering agents, such as IgG, AA, glucose, and UA (Fig. 3A). No remarkable change of current was observed in comparison with the result obtained in the presence of AFP only. Moreover, the control experiments incubated with interferences without AFP were also conducted. The results showed that the immunosensor possessed excellent selectivity for AFP.

The stability of the immunoassay system was also evaluated. When the modified electrode and the signal tag were stored in PBS (pH 6.5) at 4 °C, it retained 87.2% of its initial response after a storage period of 20 days. It suggested that the immunosensor had good stability.

3.6. Comparison of electrochemical response

In order to investigate the amplification of IL-rGO on the synthesized signal probe, a comparative study was carried by using

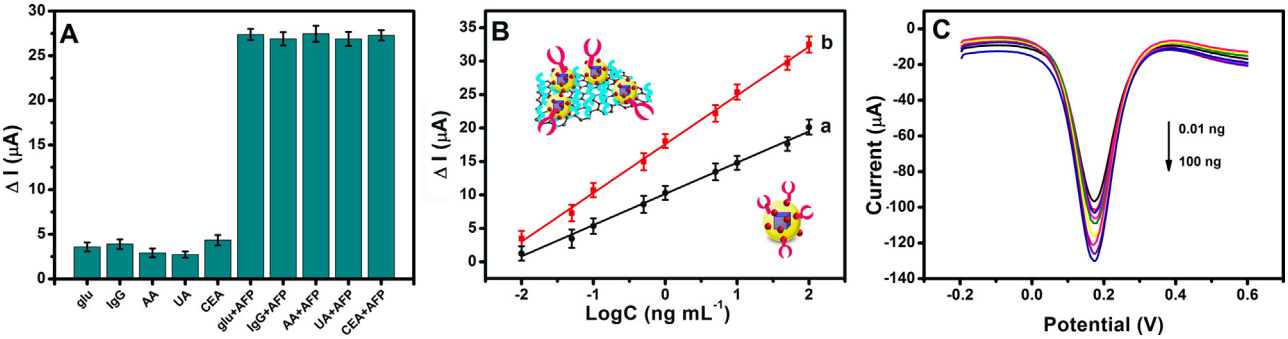

Fig. 3. (A) The selectivity of the immunosensor, (B) comparison of calibration curves of the electrochemical immunoassay used (a) Au-PDDA-PB-Ab_2 and (b) IL-rGO-Au-PDDA-PB-Ab_2 as immunosensing probe, respectively, (C) SWV response of the proposed immunosensor after incubation with different concentrations of AFP.

Table 1
Comparison of analytical properties of the developed immunosensors with other electrochemical immunosensors toward AFP.

Sensors	Linear response range ($ng\,mL^{-1}$)	Detection limit ($pg\,mL^{-1}$)	References
Au-Pd-anti-AFP	0.05–30	5	[34]
PB@HAP-HRP-anti-AFP	0.02–8	9	[4]
HRP-anti-AFP	5–80	3700	[35]
HRP-CNSs-anti-AFP	0.05–6	20	[36]
AuNPs-HRP-anti-AFP	0.25–0.45	50	[37]
SiO_2-HRP-anti-AFP	0.05–3	10	[38]
IL-rGO-Au-PDDA-PB-anti-AFP	0.01–100	4.6	This work

two kinds of signal probes as: Au-PDDA-PB-Ab_2 (a) and IL-rGO-Au-PDDA-PB-Ab_2 (b). Compared with curve a, it can be found that curve b had a higher current response under the same condition (Fig. 3B). The reason may be ascribed to the employment of IL-rGO can accelerated electron transfer.

3.7. Analytical performances of the immunsensor

Under the optimum conditions (pH 6.5; incubation time of 40 min), the dynamic range and detection limit of the proposed sensor for AFP were detected by SWV from −0.2 to 0.6 V in 0.1 M PBS (pH 6.5) containing 4 mM H_2O_2. As shown in Fig. 3C, the change currents of SWV increased with the incremental signal tags. The calibration plot showed a linear relationship in the range from 0.01 $ng\,mL^{-1}$ to 100 $ng\,mL^{-1}$ with a correlation coefficient of 0.997. The linear regression equation was $y = 7.289x + 17.594$. The detection limit for AFP reached as 4.6 $pg\,mL^{-1}$ (S/N = 3). The limit of quantitation (LOQ) was calculated to be 6.94 $pg\,mL^{-1}$ (S/N = 10). Significantly, the analytical performance of this sensor has been compared with other signal amplification methods (Table 1). As can be seen, the linear range and detection limit of the proposed immunosensor were greatly improved compared with other methods.

3.8. Analysis of clinical serum samples

The analytical reliability and application potential of the proposed method was conducted by comparing the assay results of clinical serum samples using the proposed immunosensor with the reference values obtained by enzyme-linked immunosorbent assay (ELISA). Each human serum samples was analyzed for three times. The results were shown in Table 2, and the relative errors between the two methods ranged from −2.9% to 3.5%. These results showed that there was no significant difference between the results given by two methods, indicating that the developed immunoassay could provide promising alternative tool for determining AFP in real biological samples.

Table 2
Assay results of clinical serum samples using the proposed and reference methods.

Serum samples number	Assay method and assayed concentration (mean ± SD, $n = 3$, $ng\,mL^{-1}$)		Relative error (%)
	By immunosensor	By ELISA	
1	1.95 ± 0.073	1.91 ± 0.061	2.1
2	2.09 ± 0.091	2.02 ± 0.102	3.5
3	4.51 ± 0.150	4.58 ± 0.185	−1.5
4	1.70 ± 0.059	1.74 ± 0.057	−2.3
5	1.32 ± 0.061	1.36 ± 0.053	−2.9

4. Conclusion

In this work, we successfully developed IL-rGO-Au-PDDA-PB nanocomposite which possessed high biocompatibility, conductivity and catalytic activity. A sensitive electrochemical immunosensor using the nanocomposite as label for detecting AFP was constructed and demonstrated the triple signal amplification procedure. The higher sensitivity and wider linear range of the proposed immunosensor should be attributed to the exhibition of IL-rGO and excellent electrocatalysis activities of Au-PDDA-PB. The immunosensor has excellent analytical performance with high sensitivity, good reproducibility and satisfactory storage stability. Importantly, this method can be easily expanded for detecting other relevant biomarkers and has a promising potential in clinical applications.

Acknowledgements

This research was financed by Grants from the National Natural Science Foundation of China (21273153) and Beijing Natural Science Foundation (2132008).

Appendix A. Supplementary data

Supplementary data associated with this article can be found, in the online version, at http://dx.doi.org/10.1016/j.aca.2014.04.045.

References

[1] J. Tang, D.P. Tang, R. Niessner, G.N. Chen, Analytical Chemistry 83 (2011) 5407–5414.
[2] B.V. Chikkaveeraiah, A.A. Bhirde, N.Y. Morgan, H.S. Eden, X.Y. Chen, ACS Nano 8 (2012) 6546–6561.
[3] L. Ding, J.M. You, R.M. Kong, F.L. Qu, Analytica Chimica Acta 793 (2013) 19–25.
[4] Y.X. Dai, Y.Y. Cai, Y.F. Zhao, D. Wu, B. Liu, R. Li, M.H. Yang, Q. Wei, B. Du, H. Li, Biosensors and Bioelectronics 28 (2011) 112–116.
[5] D. Lin, J. Wu, M. Wang, F. Yan, H.X. Ju, Analytical Chemistry 84 (2012) 3662–3668.
[6] X.Y. Huang, J.C. Ren, Analytica Chimica Acta 686 (2011) 115–120.
[7] Y.F. Wu, C.L. Chen, S.Q. Liu, Analytical Chemistry 81 (2009) 1600–1607.
[8] Y.F. Chang, R.C. Chen, Y.J. Lee, S.C. Chao, L.C. Su, Y.C. Li, C. Chou, Biosensors and Bioelectronics 24 (2009) 1610–1614.
[9] C. Chun, J. Joo, D. Kwon, C.S. Kim, H.J. Cha, M.S. Chung, S. Jeon, Chemical Communications 47 (2011) 11047–11049.
[10] X.M. Pei, B. Zhang, J. Tang, B.Q. Liu, W.Q. Lai, D.P. Tang, Analytica Chimica Acta 758 (2013) 1–18.
[11] Q. Gao, J.M. Han, Z.F. Ma, Biosensors and Bioelectronics 49 (2013) 323–328.
[12] F. Ricci, G. Adornetto, G. Palleschi, Electrochimica Acta (2012) 74–83.
[13] L. Ding, A.M. Bond, J.P. Zhai, J. Zhang, Analytica Chimica Acta 797 (2013) 1–12.
[14] L.J. Bai, R. Yuan, Y.Q. Chai, Y. Zhuo, Y.L. Yuan, Y. Wang, Biomaterials 33 (2012) 1090–1096.
[15] L. Yan, Y.B. Zheng, F. Zhao, S.J. Li, X.F. Gao, B.Q. Xu, P.S. Weiss, Y.L. Zhao, Chemical Society Reveiws 41 (2012) 97–114.
[16] X. Chen, X.L. Jia, J.M. Han, Z.F. Ma, Biosensors and Bioelectronics 50 (2013) 356–361.
[17] G.Q. Sun, J.J. Lu, S.G. Ge, X.R. Song, J.H. Yu, M. Yan, J.D. Huang, Analytica Chimica Acta 775 (2013) 85–92.
[18] I.V. Lightcap, P.V. Kamat, Accounts of Chemical Research 46 (2013) 2235–2243.
[19] H.M. Ma, D. Wu, Z.T. Cui, Y. Li, Y. Zhang, B. Du, Q. Wei, Analytical Letters 46 (2013) 1–17.
[20] H.C. Yang, R. Yuan, Y.Q. Chai, H.L. Su, Y. Zhuo, W. Jiang, Z.J. Song, Electrochimica Acta 56 (2011) 1973–1980.
[21] E. Nossol, A.J.G. Zarbin, Journal of Materials Chemistry 22 (2012) 1824–1833.
[22] D. Moscone, D. D'Ottavi, D. Compagnone, G. Palleschi, Analytical Chemistry 73 (2001) 2523–2529.
[23] J.H. Yang, N. Myoung, H.G. Hong, Electrochimica Acta 81 (2012) 37–43.
[24] G.F. Wang, G. Zhang, H. Huang, L. Wang, Analytical Methods 3 (2011) 2082–2087.
[25] F.Y. Kong, B.Y. Xu, Y. Du, J.J. Xu, H.Y. Chen, Chemical Communications 49 (2013) 1052–1054.
[26] J. Tang, D.P. Tang, Q.F. Li, B.L. Su, B. Qiu, G.N. Chen, Analytica Chimica Acta 697 (2011) 16–22.
[27] J. Han, Y. Zhuo, Y.Q. Chai, R. Yuan, W. Zhang, Q. Zhu, Analytica Chimica Acta 746 (2012) 70–76.
[28] E. Jin, X.F. Lu, L.L. Cui, D.M. Chao, C. Wang, Electrochimica Acta 55 (2010) 7230–7234.
[29] J.D. Qiu, H.Z. Peng, R.P. Liang, J. Li, X.H. Xia, Langmuir 23 (2007) 2133–2137.

[30] W. Zhang, L.L. Wang, N. Zhang, G.F. Wang, B. Fang, Electroanalysis 21 (2009) 2325.
[31] S.S. Kumar, J. Joseph, K.L. Phani, Chemistry of Materials 19 (2007) 4722–4730.
[32] N. Liu, Z.F. Ma, Biosensors and Bioelectronics 51 (2014) 184–190.
[33] X.B. Sun, Z.F. Ma, Biosensors and Bioelectronics 35 (2012) 470–474.
[34] T. Uemura, M. Ohba, S. Kitagawa, Inorganic Chemistry 43 (2004) 7339–7345.
[35] H.F. Yang, C.S. Shan, F.H. Li, D.X. Han, Q.X. Niu, Chemical Communications (2009) 3880–3882.
[36] Z.J. Wang, Q.X. Zhang, D. Kuehner, A. Ivaska, L. Niu, Green Chemistry 10 (2008) 907–909.
[37] L.Y. Cao, Y.L. Liu, B.H. Zhang, L.H. Lu, ACS Applied Materials & Interfaces 8 (2010) 2339–2346.
[38] L.F. Zhao, S.J. Li, J. He, G.H. Tian, Q. Wei, H. Li, Biosensors and Bioelectronics 49 (2013) 222–225.